Chemical Engineering Research and Design 200 (2023) 521–537

Contents lists available at ScienceDirect

Chemical Engineering Research and Design

journal homepage: www.elsevier.com/locate/cherd

Economic comparison of reactive distillation (RD) to a benchmark conventional flowsheet: Regions of RD applicability and trends in column design

L.J. Noll [a,*], A.G.J. van der Ham [a], S.R.G. Oudenhoven [b], A.J.B. ten Kate [b], G. Bargeman [c,d], S.R.A. Kersten [a]

[a] Sustainable Process Technology Group, Process and Catalysis Engineering Cluster, Faculty of Science and Technology, University of Twente, Drienerlolaan 5, 7522 NB Enschede, the Netherlands
[b] Nouryon, Zutphenseweg 10, 7418 AJ Deventer, the Netherlands
[c] Nobian, Zutphenseweg 10, 7418 AJ Deventer, the Netherlands
[d] Membrane Science and Technology Cluster, Faculty of Science and Technology, University of Twente, Drienerlolaan 5, 7522 NB Enschede, the Netherlands

ARTICLE INFO

Keywords:
Reactive distillation
Techno-economical assessment
Reactive tray design
Optimization
Process design

ABSTRACT

A novel methodology for the techno-economic assessment of Reactive Distillation (RD) is presented. The developed methodology benchmarks reactive distillation (RD) to a conventional reactor + distillation train flowsheet (R+D) on a cost-optimized basis, with the optimization being performed on the process unit level (reactor sizing, number of stages, feed point(s)) and the internals level (reactive tray design). This methodology is applied to the ideal quaternary system $A+B \leftrightarrow C+D$ with the conventional boiling point order of $T_C < T_A < T_B < T_D$ ($\alpha_{AD} = 4$, $\alpha_{BD} = 2$, $\alpha_{CD} = 8$). From this pool of data, a regime map of RD vs. R+D is established in which the attractive regions of either flowsheet option are identified in terms of the chemical reaction rate and chemical equilibrium. It is found that RD can arise as the cost optimal option for a large range of residence time requirements by virtue of overcoming the external recycle requirements of R+D. This is achieved through optimized reactive tray design. Contrary to conventional distillation design practices, it was found that the preferred use of bubble-cap trays over sieve trays to allow elevated weir heights and designing the column diameter below 80% of flooding become relevant design choices when accommodating high liquid holdup.

1. Introduction

Reactive distillation (RD) combines both the unit operations *reaction* and *separation* in a single column and is perhaps the most well-known example of process intensification (PI), a design philosophy that aims to reduce the energy and material usage, and thereby the costs, of the process industry by implementing multifunctional process equipment (Harmsen, 2007). The potential benefits and corresponding limitations of applying RD are already outlined in many works (Malone and Doherty, 2000; Taylor and Krishna, 2000).

The most well-known industrial application of RD is the Eastman Kodak methyl-acetate process (Agreda et al., 1990) that was developed in the 1980's. The RD process resulted in a five-fold reduction of both CAPEX and OPEX. Moreover, a significant simplification of the original flowsheet (reactor and subsequent distillation train) was realized, going from 9 to 3 process units. Other successful industrial RD processes include esterification (ethyl, butyl acetate (bypassing difficult product separations)), etherification (MTBE, ETBE, TAME (bypassing difficult feed separations)), hydrolysis, desulfurization and hydrogenation reactions, all leading to not as drastic but still significant economic benefits (Harmsen, 2007).

The successful application of RD requires a sufficient degree of overlap in the operating windows set by reaction, separation and equipment considerations (Schembecker and Tlatlik, 2003). While there is a clear beneficial effect of in-situ separation on equilibrium constrained reactions, it is key to note that RD is almost always a compromise on the operating conditions of the separate unit operations in terms of reaction and separation requirements (Baur and Krishna, 2004). This conflict of requirements also extends to column design methodology. In conventional distillation, reactions, like polymerization or cracking, are typically undesired, as they can lead to product loss or additional

* Corresponding author.
E-mail address: lionel.noll@de.sasol.com (L.J. Noll).

https://doi.org/10.1016/j.cherd.2023.10.056
Received 12 July 2023; Received in revised form 27 October 2023; Accepted 27 October 2023
Available online 2 November 2023

Nomenclature

Symbols

A,B,C,D	Fictional generic reactants and products
A_B	Tray bubbling area (m^2)
A_C	Condenser heat exchange area per heat exchanger (m^2)
$A_{C,max}$	Maximum condenser heat exchange area per heat exchanger (m^2)
$A_{C,tot}$	Total condenser heat exchange area (m^2)
A_G	Tray open area (m^2)
A_j	Vapor pressure constant
A_G/A_B	Tray open area as fraction of bubbling area (-)
A_R	Reboiler heat exchange area per heat exchanger (m^2)
$A_{R,max}$	Maximum reboiler heat exchange area per heat exchanger (m^2)
$A_{R,tot}$	Total reboiler heat exchange area (m^2)
B_j	Vapor pressure constant
B	Bottoms flow rate (mol/s)
C_l	Constant for Francis weir equation
C_p	Constant pressure heat capacity (kJ/kg)
C_{sbf}	Capacity factor for flooding calculations (m/s)
C_{tot}	Total concentration (mol/m^3)
D	Distillate flow rate (mol/s)
D_c	Column diameter (m)
D_i	Column inner diameter (ft.)
D_o	Column outer diameter (ft.)
D_T	Tray diameter (m. or ft.)
E	fractional welding efficiency (-)
F	Feed flow rate (mol/s)
F_A	Feed flow of component A (mol/s)
F_B	Feed flow of component B (mol/s)
F_{D1}	Feed flow towards column D1 (mol/s)
F_{D2}	Feed flow towards column D2 (mol/s)
f_{CAPEX}	Column cost objective function (€)
f_E	Fractional entrainment of liquid flow (mol/mol liquid)
f_{flood}	Fraction of flooding velocity (-)
f_{TAC}	Total annualized cost objective function (€/yr)
f_W	Fractional weeping of liquid flow (mol/mol liquid)
$\Delta_r H$	Enthalpy of reaction (kJ/mol)
$\Delta_{vap} H$	Enthalpy of vaporization (kJ/mol)
h_c	Clear liquid height on tray (m)
h_{da}	Downcomer apron head loss (m)
h_{dc}	Clear liquid height in downcomer (m)
h_{dt}	Dry tray head loss (m)
h_{hg}	Hydraulic gradient head loss (m)
h_{ow}	Height over weir head loss (m)
h_t	Total tray pressure head loss (m)
h_W	Weir height (m)
$h_{w,c}$	Clear liquid held by weir (m)
K_{EQ}	Chemical equilibrium constant (-)
k_f	Forward reaction rate constant (mol/mol_{Holdup} s)
L	Liquid flow rate (mol/s)
L_c	Column shell length (m)
L_W	Weir length (m)
L_{de}	Disengagement height at top of column (m)
L_{sump}	Sump height at bottom of column (m)
M_{hold}	Molar liquid holdup (mol)
M_w	Molar weight (kg/mol)
n	Exponential scaling factor of the purchasing cost with the corresponding size parameter
ΔN_s	Number of total stages relative to optimized number of total stages (-)
N_{Cond}	Number of condenser heat exchangers (-)
N_{RX}	Number of reactive stages (-)
N_s	Number of stages (-)
N_{Reb}	Number of reboiler heat exchangers (-)
P_d	Pressure vessel design pressure (psig)
P^{sat}	Saturation vapor pressure (bar)
Q_C	Condenser heat duty (J/s)
Q_L	Volumetric liquid flow rate (m^3/s)
Q_R	Reboiler heat duty (J/s)
R	Recycle flow rate (mol/s)
R_A	Reaction rate of component A (mol/s)
R_i	Reaction rate of component i (mol/s)
RR	Reflux ratio (-)
S	Maximum allowable vessel stress (psi)
$S_{F,I}$	Feed stage for component i (-)
T	Temperature (K)
T_R	Reactor temperature (K)
Tau	Residence time (s)
TS	Tray spacing (m)
t_p	Design pressure vessel thickness (in.)
t_s	Column shell thickness (in.)
t_v	Average vessel wall thickness (in.)
t_w	Necessary vessel thickness to withstand wind load (in.)
U_a	Vapor velocity through bubbling area (m/s)
U_C	Condenser heat transfer coefficient (W/m^2 K)
U_R	Reboiler heat transfer coefficient (W/m^2 K)
V	Vapor flow rate (mol/s)
V_R	Reactor volume (m^3)
W_{shell}	Column shell weight (kg)
X_i	Liquid mole fraction of component i (-)

Greek letters

α	Relative volatility (-)
$\overline{\alpha}_{ABCD}$	Set of relative volatilities for components A,B,C,D (-)
σ	Surface tension (mN/m)
μ	Viscosity (cP)
ρ	Density (kg/m^3 or lb/ft^3)
τ	Residence time (s)
ϕ_e	Effective froth density on tray (-)
$\phi_{f,dc}$	Average downcomer froth density (-)

Abbreviations

CAPEX	Capital expenditure
CSTR	Continuously stirred tank reactor
D1	Distillation column 1
D2	Distillation column 2
MESH	Mass, Equilibrium, Summation and Heat balances describing a separation stage
OPEX	Operational expenditure
PFR	Plug-flow reactor
RD	Reactive distillation
TAC	Total annualized cost (€/year)

Superscripts and subscripts

0	Initial value
F	Feed
i	Component i
j	Equilibrium stage j
L	Liquid phase
P	Product stream
tot	Total of all components
V	Vapor phase

maintenance, and have therefore been minimized via the design. The use of structured packing for separation over trays minimizes the pressure drop and liquid holdup while maximizing surface area for mass transfer (Kister et al., 2019). This mitigation of the reaction extent in conventional distillation design practices is contrary to the need for stimulating the reaction extent in RD.

Identifying RD as an attractive process option requires it to be found technically feasible (according to the combination of vapor-liquid equilibria, chemical equilibria and reaction kinetics) and economically superior to process alternatives. Several methods have been developed for assessing the feasibility of obtaining desired products from RD and the initial column lay-out. Notable examples of the feasibility analyses are the residue curve maps which consider the evaporation of a mixture accompanied by chemical reaction and the presence of distillation boundaries due to (reactive) azeotropes (Barbosa and Doherty, 1988a,b; Venimadhavan et al., 1999) and reactive distillation lines which consider a staged separation accompanied by chemical reaction at infinite reflux (Bessling et al., 1997). An extensive review of the available methods is given by Thery et al. (Thery et al., 2005; Théry-Hétreux et al., 2012). These methods can rapidly assess the feasibility of a given product split and produce an initial column layout, but can not provide details on optimal column and internals design. Furthermore, by their graphical nature, their use is limited by the number of components and the degrees of freedom in the system. Once the feasible product splits are identified, the quantitative evaluation of RD is commonly formulated as a mathematical optimization problem. Such methods consist of the following: (1) a process unit model built on first principles, (2) an economic cost function to be optimized, (3) an optimization algorithm. The process unit model contains mass, heat and vapor-liquid equilibrium relations that describe the process. Stochastic methods can use regular (reactive) distillation models as found in commercial flowsheeting software. Simulated annealing (SA) is an example of stochastic optimization algorithms and has been successfully applied to the design of RD columns (Cardoso et al., 2000; Kiss et al., 2012). Deterministic methods require the distillation model to be reformulated as a mixed-integer nonlinear problem due to the use of derivatives with respect to optimization variables. Ciric and Gu were the first to present an implementation of this method for RD (Ciric and Gu, 1994) and more recently a superstructure approach has also been used to consider auxiliary equipment together with optimal RD column design (Tsatse et al., 2021). Both of these classes of methods can be used to tackle the design problem of RD columns. Deterministic methods are computationally efficient but more difficult to implement, whereas stochastic methods are straightforward and robust but computationally expensive (Segovia-Hernández et al., 2015). Neither of these groups of methods is guaranteed to find the global optimum.

Current implementations of these methods usually model the liquid holdup on trays as the product of weir height and tray active area. The design cost for higher liquid holdup comes from increasing the weir height, and thereby the tray spacing which also increases the length of the column vessel. Two factors that are omitted by this approach are (1) the liquid froth held by the weir is significantly aerated, (2) the liquid holdup is dependent on the tray geometry and type. These methods may produce column designs that do not reach their specified productivity due to an overestimated liquid holdup. As a consequence, they do not fully capture the effect of designing for high liquid holdup on the column sizing and associated costs. Furthermore, optimized configurations of reactive internals, in terms of type and dimensioning, are only considered to a limited degree. We presented an extension of the equilibrium stage model for RD to account for the liquid holdup as a function of the tray and column design in a previous work (Noll et al., 2023). This modeling approach provides a basis to fairly compare the cost-based design of RD columns to that of flowsheets incorporating dedicated reactor units.

In this work we present a benchmarking methodology that compares RD to a conventional reactor + distillation flowsheet on a cost-optimized basis. The intended use of this methodology, in view of the overall process development timeline, is to apply it after RD has been identified as feasible (based on first principles) and its potential merit needs to be estimated before resources are allocated towards pilot testing. The desired outputs of this methodology are equipment sizing estimates and the ranking of process flowsheet options based on process economics, using limited input data (reaction kinetics, chemical equilibrium, vapor-liquid equilibrium). In a previous work, we proposed an extended reactive distillation model that directly links the equipment design to the liquid holdup (Noll et al., 2023). A similar calculation method is used here to also include the cost optimized design of reactive internals as part of the process optimization.

The key consideration in this work is whether one can economically fit a reaction into a (reactive) distillation column while achieving energy savings by overcoming chemical equilibrium. Note that the key feature of the aforementioned known implementations of RD is the solution of a separation problem rather than enhancing the reaction. Novel to this work is the attention paid to modeling the liquid holdup on reactive stages, explicitly taking into account the liquid fraction of the froth on the trays, the clear liquid height achieved by tray design, including the choice between sieve and bubble-cap trays, and the optimization of tray spacing and column diameter. The use of this methodology is shown by systematically exploring RD and the conventional flowsheet as process options for the ideal generic liquid phase reaction $A+B \leftrightarrow C+D$ with stoichiometric feed, across a wide range of chemical equilibrium constants and reaction kinetics. A single set of relative volatilities is explored here, where none of the separations between adjacent components is extremely difficult from a distillation perspective ($\alpha_{ij} = 2$) (Blahušiak et al., 2018). The results obtained allow us to quantify the limits of RD applicability for this reaction system by cost-based design i.e., economic viability rather than solely technological feasibility.

2. Methodology

The developed methodology benchmarks optimized designs of RD columns against a conventional reactor + distillation train flowsheet. Optimization is based on equipment sizing and costing with the minimized total annualized cost as the objective function. In this work we consider a quaternary chemical system with a liquid phase reaction $A+B \leftrightarrow C+D$ with ideal components. These flowsheets are economically optimized and compared for a wide range and combination of chemical equilibrium constants and forward reaction rate constants.

2.1. Scope

2.1.1. Process flowsheets

The benchmark is the conventional flowsheet employing a plug-flow reactor (PFR) and two distillation columns in a direct sequence to recover the two reaction products and recycle a combined reactant stream (see Fig. 1). Note that this is only applicable since the reactants are adjacent, middle boiling components. This layout is the most favorable according to some heuristics for sequencing of ordinary distillation columns; remove final products one-by-one as distillates, and sequence separation points in order of decreasing volatility (Seider et al., 2008). This sequencing of the distillation columns is not an inherent feature of the methodology and column sequencing optimization can readily be incorporated as an additional subroutine. The PFR was chosen as the reactor mode as this guarantees the lowest reaction volume for a positive order reaction (Levenspiel, 1999). The reactor is sized to achieve 50–99% of the equilibrium conversion, where the exact value follows from optimization between reactor size and separation throughput.

The RD flowsheet consists of a single column producing both end products at their final specifications (see Fig. 1). The column is divided into a rectifying, reactive and stripping section. Only the design of the reactive trays is optimized. The trays in the rectifying and stripping sections are sized at 0.05 m weir height with identical tray spacing as the

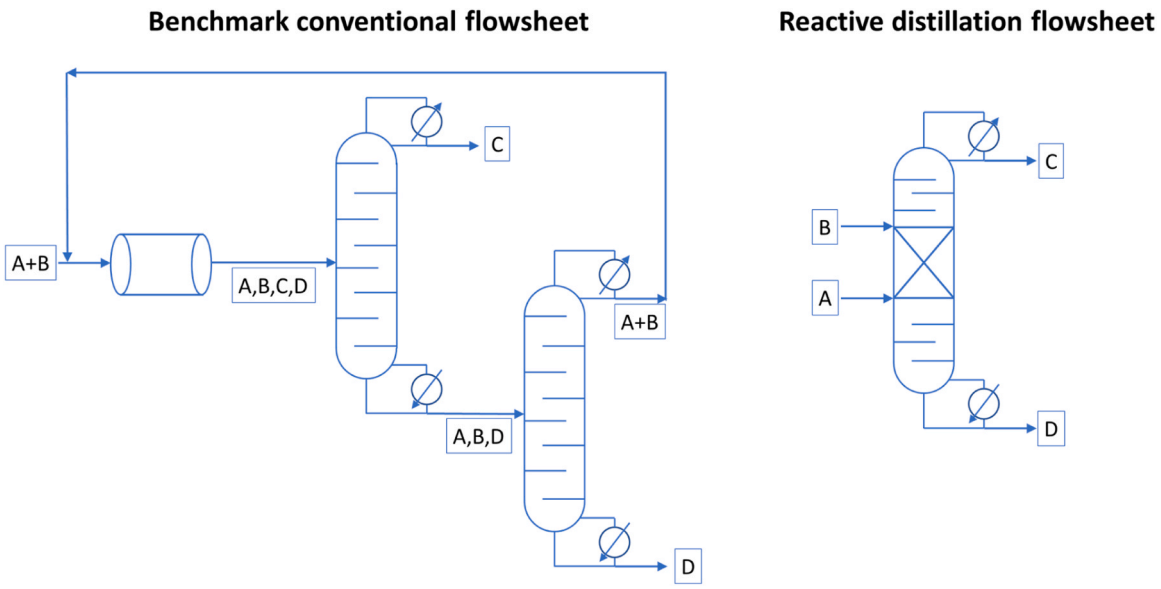

Fig. 1. Scope of the considered process flowsheets. The benchmark conventional flowsheet employs a PFR and two distillation columns in series, where unreacted A and B are recycled to the PFR. The reactive distillation flowsheet takes fresh feed of A and B and converts these to C and D to the extent imposed by the specifications. Relative volatility order: $\alpha_{CD} > \alpha_{AD} > \alpha_{BD}$.

reactive trays. The liquid holdup on the bubbling area of the trays is counted as the reactive volume, the liquid in the tray downcomer is not taken into account. Pure reactants A and B are respectively fed at the bottom and top stages of the reactive section at bubble point.

Further optimization of the feed points separately of the reactive zone sizing could be done within the methodology proposed, but is beyond the scope of this work. The reaction is set to only occur on the reactive stages i.e., between the feed points of A and B. A single value for the liquid holdup on each tray throughout the reactive zone is imposed. This assumption holds for a set of identical trays with constant V/L, negligible heat of reaction and relatively constant temperature profile and fluid properties. For systems where these properties vary significantly, a RD model which determines the liquid holdup as a function of these properties and the tray dimensions is more appropriate to account for the variations in tray-to-tray liquid holdups (Noll et al., 2023).

The top and bottom specs for all (reactive) distillation columns are summarized in Table 1. These are set to produce 99% pure C and D, with a mix of contaminants A and B, in all cases. Both flowsheets are designed to produce 20 mol/s (10 mol/s each) of products *C+D* at 99% purity, which puts it at 28.8 kta of product (assuming a molecular weight of 50 g/mol). This scale is loosely based on that used in the work of Luyben (Luyben and Yu, 2009) and would resemble the scale of a fine chemicals operation.

2.1.2. Case parameters

2.1.2.1. Reaction kinetics. The reaction rate is described by 2nd order kinetics for a reversible liquid phase reaction:

$$R_A = M_{hold} k_f \left(X_A X_B - \frac{1}{K_{EQ}} X_C X_D \right) \quad (1)$$

In this case, the forward reaction rate constant k_f and the chemical equilibrium constant K_{EQ} are taken as temperature-independent parameters. The holdup parameter, M_{hold}, is either the product of reactor volume and liquid molar density (in the case of the reactor model) or a molar liquid holdup on a given reactive tray (for RD columns).

2.1.2.2. Physical and chemical properties. An overview of the kinetic and physical parameters used is given in Table 2, most of these parameters are taken from the work of Luyben (Luyben and Yu, 2009) with some modifications and additions to establish the investigated parameter space and satisfy the parameter requirements of the hydraulic model. A set of generic values for light-medium hydrocarbons has been used for these calculations to represent an average reaction mixture. These are

Table 1
Column specifications at top and bottom. One product purity is set at one end of the column and the rest of the flow is set as a fixed flow rate at the other end, avoiding two explicit purity specs in all cases. *Implicitly sets $X_D = 0.99$.

	RD	R+D	
		D1	D2
Top spec.	$X_C = 0.99$	$X_C = 0.99$	$D = F_{D2} \times (1 - X_{D,F})$
Bottom spec.	$B = (F_B + F_A) \times 0.5$ *	$B = F_{D1} \times (1 - X_{C,F})$	$X_D = 0.99$

Table 2
Flowsheet model thermodynamic, reaction and vapor-liquid equilibrium parameters.

Parameter	Value
Heat capacity (kJ/kg K)	2
Enthalpy of formation (kJ/mol)	0
Enthalpy of vaporization (kJ/mol)	29
Molecular weight (kg/mol)	0.005
Equilibrium constant (-)	0.001 – 1,000,000 *
Forward rate constant (mol/mol_{holdup} s)	0.00032–10 * *
Pressure (bar)	1***
Vapor pressure constants $\ln(P^{sat}(bar)) = A_j - \frac{B_j}{T(K)}$	A_j B_j
A	12.34 3862
B	11.65 3862
C	13.04 3862
D	10.96 3862
α_{AD}, α_{BD}, α_{CD}	4,2,8
ρ_L (kg/m^3)	850
γ (mN/m)	30
μ (cP)	0.5

*Corresponds to equilibrium conversion of 3–99.9%. * *Corresponds to >hours - <seconds of residence time required in a PFR to approach 95% conversion. * ** Absolute pressure, applies to all process units.

assumed identical for all components, leading to identical fluid properties across the column (except for vapor density, due to T-dependence through the ideal gas law). In reality, the fluid properties can (widely) vary throughout the column based on the dissimilarity of the components, especially when water is one of the reaction products with (hydrophobic) organics as the other products. Each case is defined by a unique combination of model inputs k_f, K_{EQ}, $\bar{\alpha}_{ABCD}$ forming a single set. To eliminate any artifacts caused by temperature dependencies, the rate constants, equilibrium constant and relative volatilities (vapor pressures are equally temperature dependent) are kept constant within each case. Neither *internal* heat integration ($\Delta_r H$ is set to 0) nor *external* heat integration (no heat exchangers between streams) are included in this system. Furthermore, identical molecular weights and densities and negligible heat capacity were assumed for all components. While this is a clear simplification of real systems, this was done deliberately to prevent the results for the economic optimization of providing residence time from being clouded by a myriad of smaller, conflicting, effects.

The investigated parameter space spans equilibrium constants ranging from 10^{-3} to 10^{6} in 19 logarithmically spaced increments (3–99.9% equilibrium conversion), the lower end of this range allows the possibility of quantitatively exploring the benefit of in-situ separation with RD for very unfavorable reaction systems. The forward rate constants range from $10^{-3.5}$ to 10 in 10 logarithmically spaced increments (which reflect several hours to less than a second reaction time to approach 95 % conversion in a PFR, ignoring backwards reaction).

2.1.3. Metric for flowsheet comparison

Recognizing that RD is a less developed technology than the conventional R+D process and that costing at this preliminary stage has a significant potential error margin, it is useful to establish regions where it holds a significantly convincing (100 %+) economic advantage to make a decisive statement on where to definitely apply RD. To this end, we define the relative benefit of RD over R+D (as the benchmark) based on the total annualized cost (TAC) of each flowsheet for that specific set of parameters:

$$Rel.benefit = \left(\frac{TAC_{R+D}}{TAC_{RD}} - 1\right) * 100\% \tag{2}$$

Break-even points ($Rel.benefit = 0$), or desired relative benefit, between the two flowsheets can be calculated to establish regions within the parameter space of k_f and K_{EQ} where one flowsheet is prefered over the other.

2.2. Optimization model overview

The modeling and optimization framework applies two layers of optimization to evaluate both flowsheets for each case; an outer layer for residence time and separation capability and an inner layer for column hydraulics and internals design. An overview of this framework is shown in Fig. 2.

Flowsheet calculations are done using rigorous models implemented in MATLAB. Column calculations are performed using the inside-out algorithm and Newton's method applied to the MESH equations of the equilibrium stage model, extended for reactive distillation. Details of this model are given in a previous work (Noll et al., 2023). The reactor model is described in Appendix A. Each individual case is initialized by generating a unique set of k_f, K_{EQ} and $\bar{\alpha}_{ABCD}$ and feeding this to both flowsheets. Simulated annealing is used as the optimization routine in both levels. The used solver settings are reported in Appendix B.

2.2.1. Outer optimization level

The outer optimization level generates values for the number of stages (N_S), feed stage(s) (S_F) and reactive tray liquid holdup (M_{hold}, only for RD columns) as inputs for the flowsheet model and optimizes these variables to minimize the total annual cost of the flowsheet, posed as follows:

$$\min\{f_{TAC}(N_s, S_F, M_{hold})\} \tag{3}$$

Subject to the product purity constraints:

$$x_C^P = 0.99, x_D^P = 0.99 \tag{4}$$

And the design limits:

$$N_{S,\min} \le N_S \le N_{S,\max} \tag{5}$$

$$S_{F,\min} \le S_F \le S_{F,\max} \tag{6}$$

$$M_{hold,\min} \le M_{hold} \le M_{hold,\max} \tag{7}$$

The cost function contains a CAPEX component, based on the equipment sizing, and an OPEX component, based on the maintenance cost of the process unit(s) and the utility cost for the heat duties. The included cost items and economic relations for these components are described in Appendix C, while details on the sizing of the cost items are given in Appendix D. Table 3 lists the ranges for the outer level optimization parameters. Stages are counted from the top down, where the total condenser counts as the 1st stage and the reboiler counts as the last

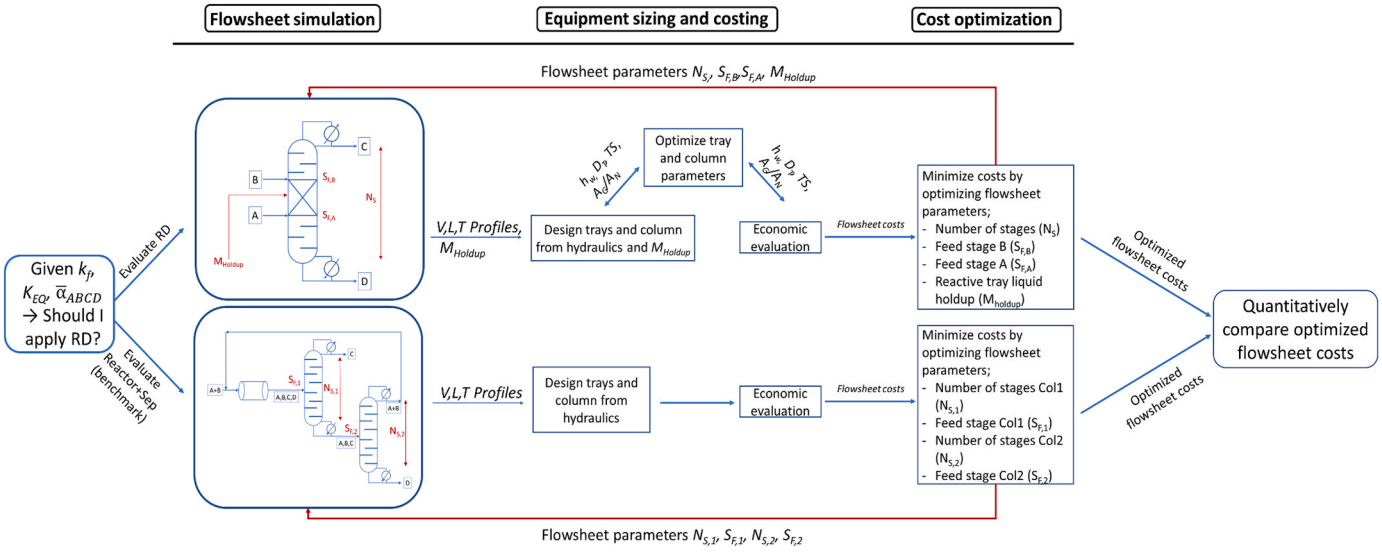

Fig. 2. Modeling and optimization framework for comparing RD to the benchmark conventional flowsheet.

Table 3
Ranges for the outer level optimization parameters for the column design.

	RD	Benchmark	
		D1	D2
N_s	15–200	10–100	10–100
$S_{F,b}$	5–60	-	-
$S_{F,a}$	10–190	-	-
S_F	-	3–95	3–95
M_{hold} (mol/tray)	200–20000	-	-
(m^3/tray)	0.012–1.17		

stage.

At each outer loop iteration, the resulting *V, L, T* profiles of the flowsheet models and imposed tray holdup are passed on to the inner optimization level for minimizing the CAPEX and the maintenance component of the OPEX. The utility component of the OPEX is determined from the heat duty calculated by the flowsheet models.

2.2.2. Inner optimization level

The inner optimization level uses the column profiles from the simulation to design a column that satisfies hydraulic feasibility i.e., stable operation on the trays while minimizing the capital cost of the column(s). This is posed as follows:

$$\min\{f_{CAPEX}(TS, f_{flood}, A_G/A_B)\} \tag{8}$$

The predicted tray liquid holdup must equal the imposed liquid holdup (for RD), subject to a minimum design weir height which presents a lower limit to the holdup:

$$(\rho_L A_B(\phi_e h_w + h_{ow} + h_{hg}))/M_w = M_{hold}, h_w \geq 0.05m \tag{9}$$

Satisfying the hydraulic stability criteria [7]:

$$entrainment: f_E \leq 0.1 \tag{10}$$

$$downcomer \quad backup: h_{dc}/\phi_{f,dc} \leq TS \tag{11}$$

$$weeping: f_W \leq 0.1 (\text{sieve trays } only) \tag{12}$$

and the tray design parameter limits:

$$Tray \quad param._{\min} \leq Tray \quad param. \leq Tray \quad param._{\max} \tag{13}$$

Table 4 lists the ranges for the tray design parameters at the inner optimization level. Minimization of the column capital cost is achieved by optimizing the open area, tray spacing and design approach to flooding (fixed at 80 % for normal distillation, variable for RD) for the trays, as well as choosing between sieve and bubble-cap trays. Weir height is optimized implicitly as it follows from the other tray design parameters and the imposed liquid holdup from the outer optimization level. An overview of the hydraulic model equations and implementation is given in Appendix E. All reactive trays are assumed identical in terms of design parameters except for the weir height, which varies slightly due to each tray having a different froth density as a result of the temperature profile. In practice, columns will usually have a single set of reactive trays with constant weir height due to construction cost considerations, resulting in slight differences in liquid holdup from tray-to-tray.

The bubble-cap trays represent a specialized design alternative to using sieve trays, with greater flexibility in terms of achieving high liquid holdups, albeit at a higher cost. This flexibility comes from the possibility to design column diameter well below the typical 80% of (entrainment) flooding vapor velocity as a means of creating additional liquid holdup to satisfy residence time requirements. This has the two-fold benefit of increasing the space available for liquid holdup *and* increasing the froth density by lowering vapor velocity. Weeping on sieve trays limits this design option as sufficient vapor velocity is needed to prevent the liquid holdup from significantly seeping through the holes. Weeping also limits the allowable maximum weir height as a increased liquid height also increases the degree of weeping. Bubble-cap trays by their design are not hindered by these phenomena.

3. Results and discussion

The developed methodology benchmarks reactive distillation (RD) to a conventional reactor + distillation train flowsheet (R+D) on a cost-optimized basis, with the optimization being performed on the process unit level (reactor sizing, number of stages, feed point(s)) and the internals level (RD only, reactive tray design). The following sections show the results of applying this methodology to the ideal quaternary system $A + B \leftrightarrow C + D$ with the conventional boiling point order of $T_C < T_A < T_B < T_D$ ($\alpha_{AD} = 4$, $\alpha_{BD} = 2$, $\alpha_{CD} = 8$).

3.1. Economic comparison of reactive distillation and the benchmark reactor + separation train

The primary goal of this methodology is to identify opportunities for applying RD, given a set of system characteristics: the forward reaction rate constant k_f, chemical equilibrium constant K_{EQ} and the set of relative volatilities $\overline{\alpha}_{ABCD}$. Fig. 3 shows the k_f - K_{EQ} field, for a single set of relative volatilities, with the 100% relative benefit – and break-even point contour lines. To give a tangible interpretation for the range of k_f values, the right-hand y-axis gives equivalent values for the residence time required in a PFR to reach 95 % total conversion (considering only the forward reaction and with a stoichiometric feed of A and B) along the k_f scale.

The break-even line (red line) from Fig. 3 shows that for the evaluated case ($\alpha_{AD} = 4$, $\alpha_{BD} = 2$, $\alpha_{CD} = 8$) RD is always the cheaper option when the reaction is sufficiently limited by chemical equilibrium ($K_{EQ} < 10^{-1}$, 24% single-pass conversion). For more mildly equilibrium limited reactions ($K_{EQ} = 10^{-1}$-10^{4}, 24–99 % single-pass equilibrium conversion) the reaction rate determines whether RD (higher k_f) or R+D (lower k_f) is preferable. A favorable chemical equilibrium ($K_{EQ} > 10^{4.5}$, >99 % single-pass equilibrium conversion i.e., product specification is reached without external recycle for R+D) results in RD being either only marginally better or outperformed by R+D in process economics. It has to be kept in mind that the studied volatility order $\alpha_{CD} > \alpha_{AD} > \alpha_{BD}$ is the most favorable case for RD (Tung and Yu, 2007) and that the assumed relative volatilities represent a relatively easy separation process (Blahušiak et al., 2018). The results shown here therefore do not reflect the potential benefit of RD to overcome difficult separations by converting some of the components. The 100 % relative benefit line is similar to the

Table 4
Ranges for the inner level optimization parameters for the tray design.

Design param.	Symbol	Units	Range	Related hydraulic phenomena	Notes
Tray spacing	*TS*	m	0.4 * –0.9 m. (16–36 in.)	Entrainment, downcomer backup flood	Set either by entrainment over the bubbling area or the downcomer backup.
Fraction of flooding	f_{flood}	(-)	0.4–0.8	Entrainment, weeping	Sets the column diameter.
Tray open area	A_G/A_B	(-)	0.08–0.14	Weeping, downcomer backup flood	Sets the vapor velocity through the disperser unit.

*Rounded up from 0.38 m since optimization designs tray spacing in 0.05 m increments.

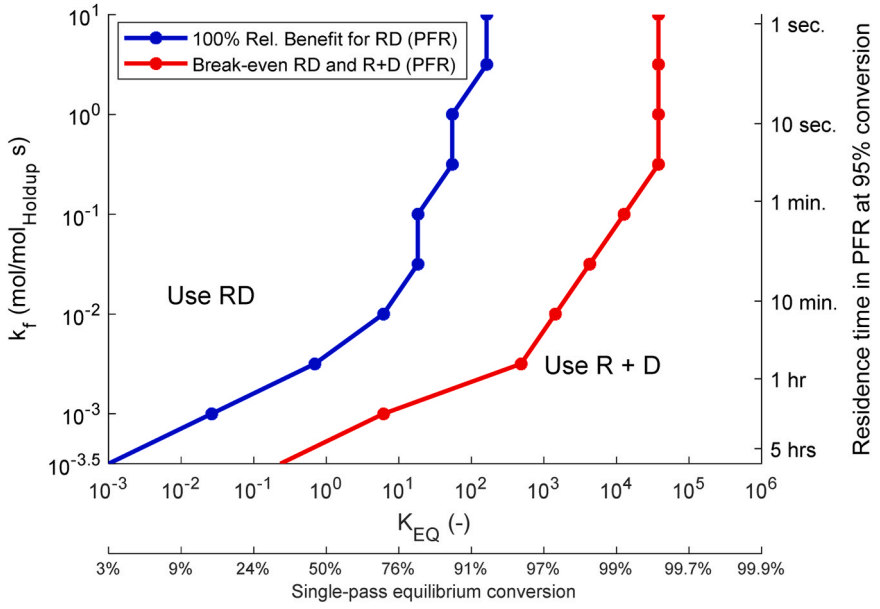

Fig. 3. Comparison of RD to conventional flowsheet based on process economics. Contour line of 100% economic benefit for RD (left). Contour line of break-even for RD and R+D (right). $\alpha_{AD} = 4$, $\alpha_{BD} = 2$, $\alpha_{CD} = 8$. Production of 28.8 kta of C+D (14.4 kta each). X-axis indicate values for K_{EQ} and their equivalent single-pass conversions at stoichiometric feed of A and B. Y-axis indicate values for k_f and their equivalent residence time to reach 95% absolute conversion in a PFR in the absence of backwards reaction.

break-even line, but shifted along the K_{EQ} axis. Until $K_{EQ} = 10^1$, the vertical difference is one order of magnitude in k_f, where for higher K_{EQ} this difference increases. The total process costs decrease towards higher K_{EQ} for both flowsheets and are proportionally more dependent on the required residence time (reactor volume or number and size of reactive stages). The increasing difference in k_f between the two contours is due to reactive volume being more costly to provide in an RD column than in a pure liquid phase PFR. Reactive distillation being applicable to equilibrium-limited reactions that do not have excessive residence-time requirements is well-known conceptually (Taylor and Krishna, 2000). The presented methodology quantifies these aspects in terms of total process costs for a given reaction system. Furthermore, the relative benefit contours also indicate whether it is worthwhile investigating the process development of RD in more detail. To explain the obtained result, the following sections considers several characteristics and design aspects of both process flowsheets.

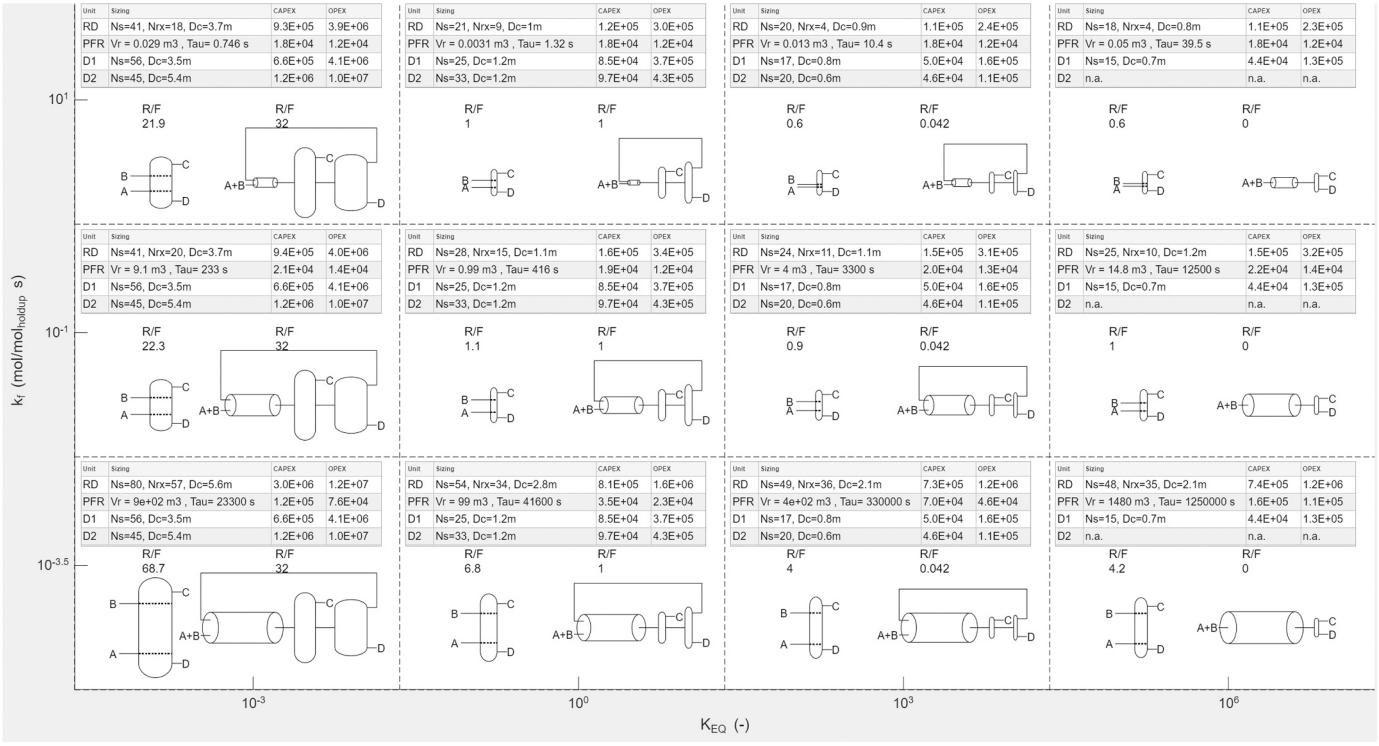

Fig. 4. Optimized R+D and RD designs for selected cases. X and y axis indicate the k_f and K_{EQ} values for the individual cases. The (reactive) distillation columns are scaled relative to each other. PFR is scaled relative to itself. Reported values for CAPEX and OPEX are annualized.

3.2. Optimized flowsheet designs

3.2.1. Placeholder

The optimization of RD and R+D for a wide range of K_{EQ} and k_f has produced a large set of flowsheet designs. A selection of these cost optimized designs within the investigated parameter field is shown in Fig. 4. To provide a visual comparison of the optimized flowsheet designs the distillation columns for the R+D option and RD columns are drawn to scale with each other in terms of the number of stages and column diameter. The reactor size for the R+D option is only to scale relative to itself, not to the columns. Additionally, sizing and costing data of the individual units are provided.

The R+D designs are the most straightforward to interpret. For $k_f = 10^1$, across the entire range of K_{EQ}, the size of the reactor (PFR) is very small. It should be noted that the cost correlations for all process units follow the form $\boldsymbol{y = a + b * size\ parameter^n}$, which consists of a fixed and a variable component of the purchasing cost. This results in even the very small units having at least the fixed portion ($\boldsymbol{a}$) of the capital investment cost. Moving down to $k_f = 10^{-3.5}$, the reactor increases vastly in size, becoming a significant contributor to the total costs. The left side of Fig. 4 represents the severely chemical equilibrium limited cases. As expected, the R+D flowsheet has a significant recycle stream to meet the conversion demands of the feedstock, as evidenced by the high recycle to feed (R/F) ratios. This recycle stream requires the distillation columns to process a large amount of material, hence the size of the columns in terms of number of stages and column diameter being the largest for these cases. Moving towards the right side of the figure (higher K_{EQ}), the recycle decreases and with it the size of the distillation columns. The residence time of the liquid inside the reactor increases from low to high K_{EQ}, but the volume of the reactor passes through a minimum. At low K_{EQ} (the far left of Fig. 4) the reactor sizing is due to the amount of material passing through, whereas at high K_{EQ} (the far right of Fig. 4) the high degree of conversion in the reactor, and thus the residence time requirement dictates the reactor size. The R+D designs at $K_{EQ} = 10^6$ feature only a single distillation column, as the product specifications can be met in a single pass due to the effectively irreversible reaction.

The RD column designs share features with R+D regarding how the design accommodates varying degrees of K_{EQ} and k_f. In most optimization studies the RD column diameter is related to the reflux ratio at a fixed approach to (entrainment) flooding velocity. Since in this work the design approach to flooding was used as a separate optimization parameter, the resulting column diameters are an additional result. Some discernible trends that have already been reported in literature can be identified (Muthia et al., 2018):

- As the reaction rate or chemical equilibrium constant decreases, the number of reactive stages increases.
- The reflux ratio increases (steeply) for lower values for the chemical equilibrium constant.

An important difference is seen in how the cost-optimized design of an RD column accommodates low reaction rates compared to R+D. When the forward reaction rate k_f decreases (going from top to bottom in Fig. 4) the *internal* recycle in the RD column, and with it the diameter, increases. For R+D however, the *external* recycle, and with it the distillation column sizing, stays constant and only the reactor increases in size. As will be discussed in more detail in Section 3.3, incorporating a high residence time in an RD column is costly due to the small liquid fraction of the total volume in the column. Pulling the equilibrium to the product side by removing component C boosts the productivity of the liquid present on the trays by operating farther from chemical equilibrium. Hence, the cost-optimized designs of these RD columns feature an increased reflux ratio to accommodate lower reaction rates. In contrast, for R+D pursuing chemical equilibrium at the outlet of the plug-flow reactor is cheaper than settling for partial conversion and increasing the sizing of the distillation train to compensate.

The economic flowsheet comparison shown in Fig. 3 identifies a threshold for K_{EQ} where R+D is cheaper than RD, regardless of the reaction kinetics. The right side of Fig. 4 visualizes this result for a case where $K_{EQ} = 10^6$: a single-pass R+D configuration, allowing for a single distillation column and avoiding the recycle, is always cheaper than the corresponding RD column. This makes sense from both the separation and the reaction perspective. The RD column separates component C from A/B/D in the rectifying section and component D from A/B/D in the stripping section, whereas the single distillation column only separates C from D, which is by definition the easier separation for the boiling point order studied. Additionally, an increase in liquid holdup requires a 5–20 times higher increase in column volume compared to the increase in (liquid phase) reactor volume. For all cases where $K_{EQ} \leq 10^4$, this model system requires a recycle for R+D, and therefore two distillation columns. Whether the integrated option (RD) or the non-integrated option (R+D) is preferable boils down to whether the gains of overcoming chemical equilibrium are outweighed by the costs of (inefficiently) designing for high liquid holdup.

Finally, the most extreme RD column designs are found for the combination of low K_{EQ} and low k_f, where both a significant column diameter (due to a high reflux ratio) and a high number of reactive stages (due to very high residence time requirements) are found. By themselves, these are the column designs that could lead the designer to move away from considering RD as a preferable option since the reflux ratio is very high for a distillation column. Considering the economic comparison in Fig. 3 however shows that the most extreme RD column designs do not guarantee the most unfavorable position relative to the benchmark process. This highlights that the choice of whether to consider RD or not cannot be made solely from the initial, or optimized, design of an RD column and comparing these to 'acceptable' values for number of stages or reflux ratio, but has to be made relative to some other benchmark flowsheet option.

3.2.2. Sensitivity of optimized RD columns

The use of simulated annealing for the optimization does not guarantee finding the global optimum. However, it was seen that similarly to conventional distillation columns, the RD columns showed relatively flat cost optima at a sufficient distance from the minimum stages asymptote. The sensitivity of the TAC of RD column designs with respect to the total number of stages near their optimized values is shown in Fig. 5. These data points were obtained by perturbing the optimal number of stages by a fixed value (−5 to +5) and optimizing the feed stages and liquid holdup i.e., every data point is a new cost-optimized RD column design at a fixed total number of stages.

Relative to the optimal number of stages ($\Delta N_s = 0$), adding more stages increases the CAPEX (larger column shell, additional trays) and lowers the OPEX (lower reflux ratio to meet the same specifications). The lower reflux ratio also affects the CAPEX to a lesser degree due to the smaller heat exchangers and smaller column diameter but this is offset by the other capital cost components i.e., increased column height and additional trays. Inversely, reducing the number of stages increases the OPEX but decreases the CAPEX. Overall, within a decent range of RD column designs, very similar values of the TAC are obtained.

3.3. Tray and column design

The model used in this work optimizes tray spacing, diameter (through f_{flood}), tray open area (sieve trays only) and tray type (sieve/bubble-cap), and by extension also the weir height, to minimize the CAPEX of the designed columns. This section shows the design trends that follow from the optimization and to establish regions within the k_f-K_{EQ} field where certain characteristics for the column design dominate.

Fig. 6 shows the choice of tray type and f_{flood} made by the optimization in the k_f-K_{EQ} field. It can be concluded that there is a significant region for low to medium k_f where bubble-cap trays are optimal, due to the need for additional liquid holdup, where bubble-cap trays have the

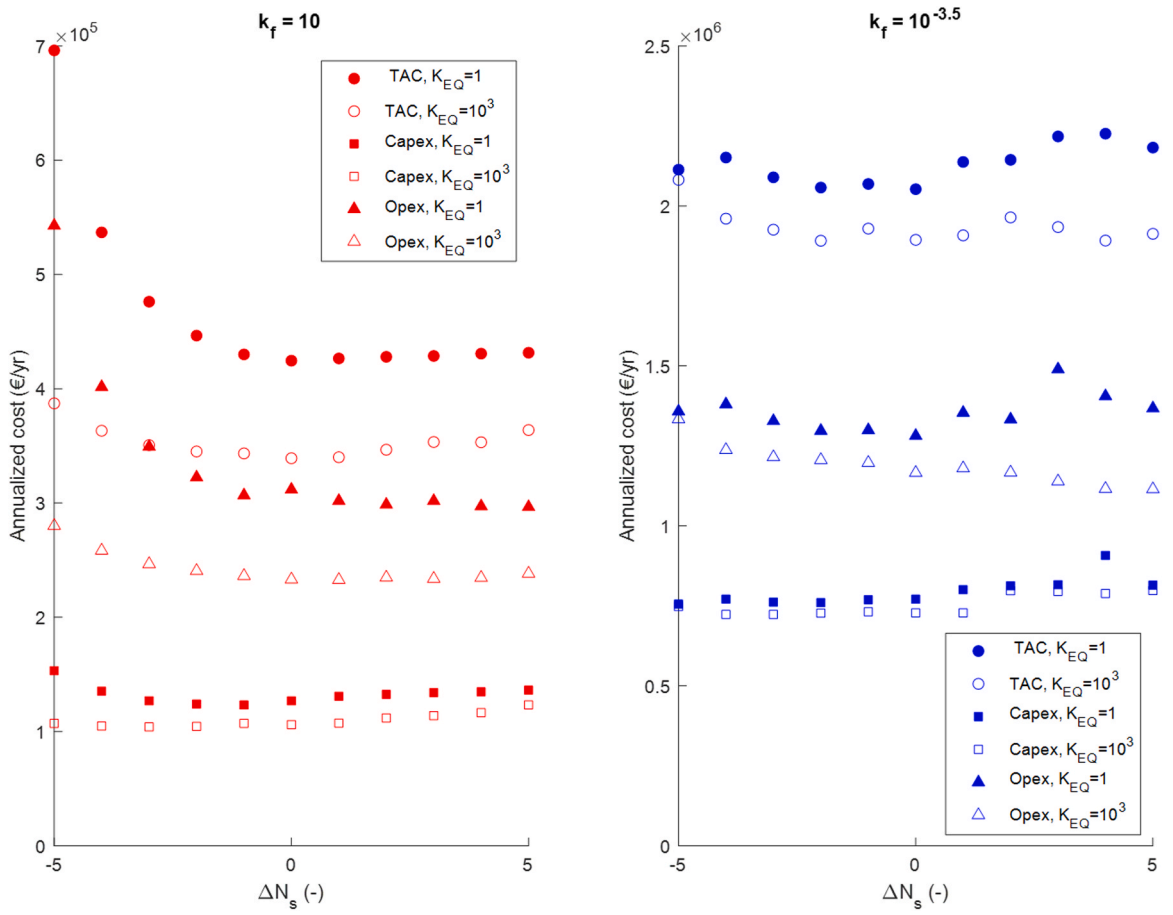

Fig. 5. Sensitivity of the TAC of RD columns to the total number of stages. Feed stages and liquid holdup are optimized at a fixed number of total stages for these RD columns.

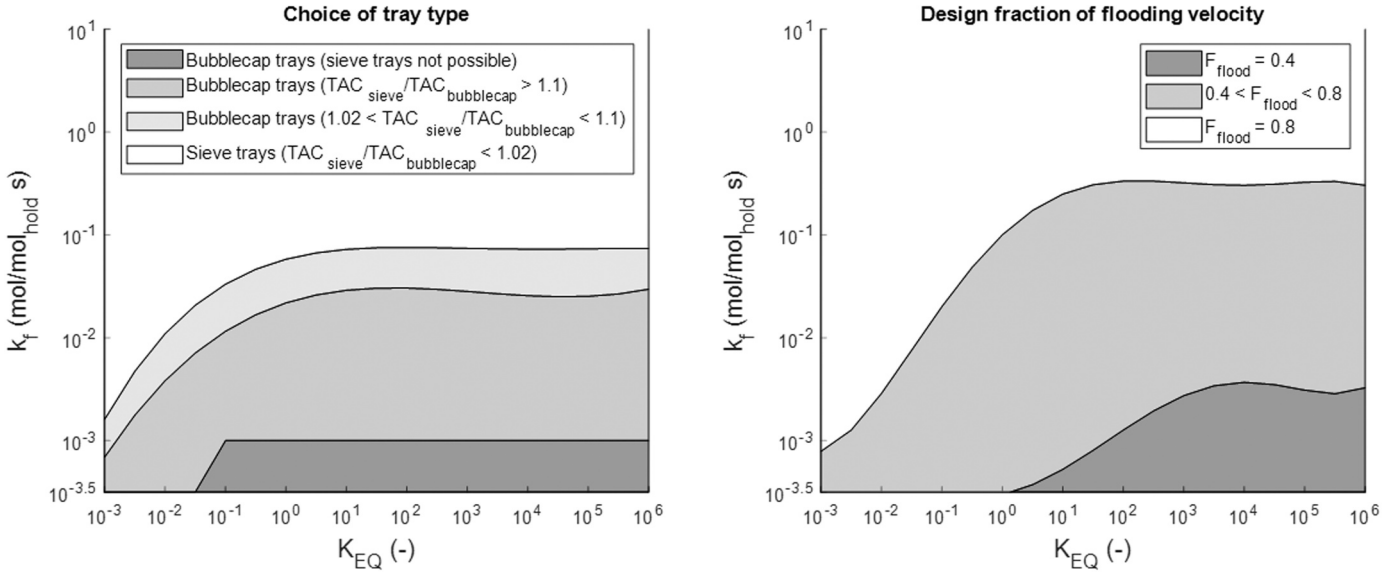

Fig. 6. Choice of tray type (left) and fraction of flooding (right) for the optimized RD columns. Lower bound of $TAC_{sieve}/TAC_{bubblecap}$ was found to be 0.98.

benefit of a higher froth density compared to sieve trays and can operate at lower f_{flood}. The tray choice becomes increasingly important towards lower k_f, with the highest relative cost within the optimized cases of this work being 1.3. A region of very low k_f is observed where no feasible RD column design is found for sieve trays within the specified optimization limits for total number of stages (120 stages).

Deviating from the standard $f_{flood} = 0.8$ is found to be optimal in a significant part of the k_f-K_{EQ} field and coincides with the cases where bubble-cap trays are optimal. Sieve trays run into weeping limitations when lowering f_{flood}. At low K_{EQ}, the upper boundary of $f_{flood} = 0.8$ is

optimal, for the majority of the range in k_f. RD columns designed for low K_{EQ} have a high diameter, due to the high reflux needed. This inherently solves part of the holdup requirements, where further increasing the column diameter is not optimal from a process economic perspective. Towards higher K_{EQ} however, the column diameter was deliberately increased by lowering f_{flood} i.e., moving away from the lowest possible diameter. In some cases, f_{flood} was lowered all the way down to the lower boundary of 0.4, characterized by cases with low k_f and higher K_{EQ}. This design choice has a two-fold benefit for providing liquid holdup as both the physical space for the liquid pool is increased *and* the liquid fraction of the liquid pool is increased.

Table 5 shows the optimized reactive tray designs for the cases shown in Fig. 4. For high k_f the difference between sieve and bubble-cap trays is marginal and is attributed to the internals comprising only a small fraction of the TAC, paired with the performance of these columns being relatively insensitive to the liquid holdup due to the high intrinsic reaction rate. The lowest attained value for $TAC_{sieve}/TAC_{bubblecap}$ was found to be 0.98, owing to the column internals amounting to only several percent of the total column CAPEX. Primarily towards lower k_f (due to slower reaction rate), but also towards higher K_{EQ} (due to higher attainable conversion), bubble-cap trays have an increasingly larger cost advantage due to enabling less reactive trays for the same liquid holdup, which follows from the liquid fraction (φ_e) being consistently higher for bubble-cap trays. Several cases for $k_f = 10^{-3.5}$ are infeasible with sieve trays due to limited design flexibility in both liquid height (weir height) and bubbling area (f_{flood}) without running into weeping limitations. Bubble-cap trays have a wider design space in these regards, with the most extreme designs in this work showing weir heights of 0.3 m and $f_{flood} = 0.4$. These trays are designed at the highest possible liquid holdup achievable within the imposed ranges of the tray design parameters.

By considering the tray dimensioning in the optimization, it is possible to quantitatively distinguish attractive internal types and design choices for RD columns that fall outside of common distillation design practices, which are found here at low k_f values.

4. Conclusion

A benchmarking methodology was established to provide the cost-optimized design and evaluation of reactive distillation (RD) vs. alternative flowsheets. In this work RD was benchmarked against a conventional reactor + distillation configuration (R+D). The methodology was applied to a generic equilibrium limited liquid phase reaction using reactants A and B and generating products C and D with the conventional boiling point order of $T_C < T_A < T_B < T_D$. Special attention was given to ensure that the required liquid holdup can be located on the tray by proper tray design. Quantitative results for a single set of relative volatilities ($\alpha_{AD} = 4$, $\alpha_{BD} = 2$, $\alpha_{CD} = 8$) have been generated with this methodology. Based on these results clear regions for preferred process configuration options were established in terms of the key forward reaction rate constant k_f and equilibrium constant K_{EQ}.

While RD can be regarded as a poor reactor in terms of liquid volume, it also provides a significant benefit by means of the simultaneous in-situ separation of the low boiling product from the mixture, enhancing reactions that are limited by chemical equilibrium. Overcoming the external recycle requirement of R+D outweighed the costs of accommodating higher residence time requirements for RD for many cases. Optimization of the reactive internals has shown that the deliberate choice of bubble-cap trays over sieve trays and lowering of f_{flood} are important design options below a certain forward reaction rate constant (0.1 s^{-1}), as designs with > 10 % lower cost were obtained for RD with bubble-cap trays compared to those with only sieve trays.

Low equilibrium constants, equivalent to 25 % or lower single-pass conversion, favor RD. This can be understood since the rate of internal recycle (reflux) of these columns is considerably less than the external recycle rate for the conventional reactor + distillation train. High equilibrium constants (75–9 9% single-pass conversion) paired with a sufficiently high forward reaction rate constant (0.1 s^{-1}) also favor RD although at a lesser degree. This is due to the number of process units being reduced from three to one. However, at lower reaction rate constants and the relatively high equilibrium constants in this range, liquid holdup needs to be increased by altering tray design and adding reactive stages, leading to RD designs that are more costly than the conventional flowsheet. If the equilibrium constant (> 99 % single pass conversion) is high enough to meet product specifications in a single pass i.e., allowing for a two-unit (reactor + one distillation column) flowsheet without external recycle, then it is found to always be cheaper than RD.

Funding

This research was funded through project ReaDi for which funding was provided by Nouryon and Nobian Industrial Chemicals B.V. (formerly AkzoNobel Chemicals International B.V.).

Declaration of Competing Interest

The authors declare that they have no known competing financial interests or personal relationships that could have appeared to influence the work reported in this paper.

Table 5
Reactive tray designs for several optimized RD columns. Optimized column designs can differ (number of stages, feed stages, liquid holdup) between tray types for the same case. Relative TAC is defined as $TAC_{sieve}/TAC_{bubblecap}$.

		Sieve trays				Bubble-cap trays				
k_f	K_{EQ}	f_{flood} (-)	TS (m)	h_w (m)	φ_e (-)	f_{flood} (-)	TS (m)	h_w (m)	φ_e (-)	Rel. TAC
10	10^{-3}	0.8	0.4	0.057	0.34	0.8	0.4	0.059	0.52	0.999
	10	0.8	0.4	0.068	0.36	0.7	0.4	0.058	0.55	0.989
	10^3	0.8	0.4	0.086	0.41	0.7	0.4	0.094	0.56	0.988
	10^6	0.8	0.4	0.06	0.36	0.7	0.4	0.058	0.55	0.982
$\mathbf{10^{-1}}$	10^{-3}	0.8	0.4	0.056	0.34	0.8	0.4	0.058	0.52	1.000
	10	0.8	0.4	0.079	0.38	0.7	0.4	0.1	0.56	1.027
	10^3	0.8	0.4	0.077	0.4	0.6	0.4	0.11	0.59	1.037
	10^6	0.8	0.4	0.076	0.4	0.6	0.4	0.11	0.59	1.046
$\mathbf{10^{-3.5}}$	10^{-3}	0.8	0.45	0.1	0.39	0.7	0.6	0.14	0.51	1.121
	10	-	-	-	-	0.4	0.6	0.18	0.57	-
	10^3	-	-	-	-	0.4	0.9	0.31	0.59	-
	10^6	-	-	-	-	0.4	0.9	0.31	0.59	-

Appendix A. MATLAB flowsheet model details

The developed MATLAB model performs rigorous calculations for distillation and reaction (PFR using an n-CSTR in series approach) using an equation-oriented approach.

Distillation model equations

The distillation model uses the equilibrium stage model as outlined by Naphtali and Sandholm (1971), extended to include liquid phase reaction, details of the implementation of this model are given in a previous work (Noll et al., 2023). The liquid holdup is imposed by the optimization routine and the tray parameters are adjusted to achieve the given liquid holdup. This approach treats the tray and column sizing as a post-processing step of the column simulations.

Reactor model equations

The reactor model describes a PFR by using a cascade of 7 adiabatic CSTR's. The individual CSTR models consist of algebraic mass balances and a heat balance to account for the transformation of chemical components and generation/consumption of heat through reaction.

$$M_i = 0 = l_i - Fx_{i,F} - R_i \tag{A.1}$$

$$H = 0 = T_R - T_F \tag{A.2}$$

In this work it is assumed that the specific heat of all components is identical, the reaction has a net molar consumption of zero and no additional heat is added to the reactor. The result is that the full energy balance based on enthalpy reduces to the temperature balance given by equation A.2.

Appendix B. Simulated Annealing solver settings

Simulated Annealing (SA) is a metaheuristic search strategy for approaching global optimization. It is a probabilistic method technique which is useful for finding approximate optima, especially when the search space is discrete. Optimizing down to individual euros would prefer a discrete method, however this requires calculation of derivatives and more importantly from a process design standpoint be a level of accuracy that loses its meaning considering the approximate nature of cost assessment. Hence, we may do with this approximate approach. The column design problem is largely characterized by discrete decision variables i.e., number of stages, feed stages. While tray liquid holdup is technically a continuous parameter, it has been discretized in 50 mol increments to comply with SA. Again, optimizing towards individual moles of tray liquid holdup would imply an accuracy that exceeds that of the design equations used (hydraulic model) and it was deemed appropriate to use this approximate approach. Similarly, the design variables of the hydraulic model were discretized to limit the search space and comply with this optimization method. These parameters were enforced to be integers by rounding, where iterations for which the rounded set of variables matched an already evaluated point were rejected and restarted.

Simulated annealing mimics the physical annealing process from metallurgy, where the system moves towards minimum energy as its temperature decreases. The defining optimization settings are the form of the annealing function, form of the temperature function, starting temperature, reannealing interval, maximum number of iterations and maximum number of stall iterations. The 'atoms' or variables that make up the system have a greater kinetic energy at higher temperature giving them a higher mobility. The optimization equivalent of this principle is that the maximum step size that a variable can make between iterations is proportional to the current temperature, where in this work the built-in function @annealingboltz is used:

$$\Delta X_{\max} = \sqrt{T} \tag{B.1}$$

With each new iteration, the temperature is progressively lowered i.e., 'cooling' occurs. Here, @temperatureboltz is used:

$$T = \frac{T_0}{\log(k)} \tag{B.2}$$

Note that each optimization variable has its own (starting) temperature.

The annealing parameter k is a proxy for the iteration number i.e., time of the annealing process. A reannealing interval can be specified where after a certain number of iterations the annealing parameter is reset to its initial value, raising the temperature again. Reannealing causes the step length to increase again, enabling this technique to escape local minima. Simulated annealing also offers the option to accept a point with a higher 'energy' or function value, with a probability determined by a pre-set acceptance function which also enables escaping local minima. This functionality is not used in this work. The number of iterations should be chosen high enough to give some guarantee of optimality. The maximum number of stall iterations sets a limit to how many successive iterations are performed where no new best point is found, where it is likely that global optimality has already been reached. The values for the number of iterations used in this work are based on our own experience. Tables B-1 and B-2 list the optimization settings and parameters used for the RD column, distillation column and hydraulic column optimizations.

At each iteration of the outer optimization a set of $N_{stages} \times (2NC+1)$ nonlinear equations is solved for each (reactive) distillation column and $N_{CSTR} \times (2NC+1)$ nonlinear equations for the PFR (approximated by 7 CSTR's in series). These equations are solved by Newton's method for the same number of variables (l, v, T) i.e., the system is square. The subsequent sizing and costing consist of a series of algebraic equations that are solved at each iteration of the inner optimization.

Table B-1
Optimization parameter settings used with Simulated Annealing. *only applicable to sieve trays.

RD column		
Type	Range	Increment
N_s	10–120	1
$S_{F,A}$	5–20	1
$S_{F,B}$	6–110	1
M_{hold}	200–20000	50 mol
Distillation column		
Type	**Range**	**Increment**
N_S	10–120	1
S_F	5–115	1
Hydraulic design		
Type	**Range**	**Increment**
f_{flood}	0.4 – 0.8	0.1
TS	0.4 – 0.9 m	0.05 m
A_G/A_B*	0.08 – 0.14	0.01

Table B-2
solver settings used with Simulated Annealing. *only for sieve trays.

RD column	
Type	Setting
Temperature function	$T = \frac{T_0}{\log(k)}$
Annealing function	$\Delta X_{max} = \sqrt{T}$
T_0	[10 10 10 100]
Reanneal interval	30
Max. Number of iterations	500
Max. Number of stall iterations	250
Distillation column	
Type	**Setting**
Temperature function	$T = \frac{T_0}{\log(k)}$
Annealing function	$\Delta X_{max} = \sqrt{T}$
T_0	[10 10]
Reanneal interval	30
Max. Number of iterations	300
Max. Number of stall iterations	250
Hydraulic design	
Type	**Setting**
Temperature function	$T = \frac{T_0}{\log(k)}$
Annealing function	$\Delta X_{max} = \sqrt{T}$
T_0	[20 20 20 *]
Reanneal interval	5
Max. Number of iterations	600
Max. Number of stall iterations	-

Appendix C. Economic sub-model

Mathematically, the column design is posed as a minimization of the column cost function. The column cost is the sum of the column shell, tray, reboiler and condenser (heat exchanger) costs. Additionally, the reactor is also included as a cost item for the conventional flowsheet. These costs are calculated by the economic relations of Coulson and Richardson (Lucia, 2008), shown in Table 8. The determination of the weight of the distillation column shell and heat exchanger areas is outlined in Appendix D.

Table 8
Flowsheet cost items and costing formulas, based on values from 2010 in dollars [26].

Cost item	Symbol	Additional information	Cost relation
Distillation column (shell)	C_{DC}	Vertical pressure vessel, stainless steel	$C_{DC} = 17400 + 79 * (W_{shell}(kg))^{0.85}$
Trays	C_T	Sieve (bubble-cap at 2x price) trays, stainless steel (per tray)	$C_T = 130 + 440 * (D_T(m))^{1.8}$
Reboiler	C_R	U-tube kettle reboiler	$C_R = 29000 + 400 * (A(m^2))^{0.9}$
Condenser	C_C	U-tube shell and tube	$C_C = 28000 + 54 * (A(m^2))^{1.2}$
Reactor	C_{RC}	Jacketed, agitated, stainless steel	$C_{RC} = 61500 + 32500 * (V(m^3))^{0.8}$
Steam	C_{OS}	No differentiation between grades	€24/ton

The purchasing cost of either flowsheet is determined by summing the relevant cost components and indexing this value for the current cost, in 2017, by the CEPCI (Chemical Engineering Plant Cost Index) compared to its 2010 value:

$$C_{purchase,bare} = \frac{CEPCI_{2017}}{CEPCI_{2010}} * \sum_{i=1}^{n} C_i = \frac{567.1}{533} * \sum_{i=1}^{n} C_i \tag{C.1}$$

Additionally, the purchasing cost is multiplied by a Lang factor (4 for a fluid processing plant) to account for installation.

$$C_{purchase} = C_{purchase,bare} * 4 \tag{C.2}$$

These capital costs are annualized by assuming a 15% interest rate and a plant life time of 15 years:

$$CAPEX \quad \left(\frac{\$}{yr}\right) = C_{purchase} * \frac{interest}{\left(1 - (1 + interest)^{-plant \quad life}\right)} \tag{C.3}$$

Finally, costs are converted to euros based on the exchange rate of dollars to euros (0.9):

$$CAPEX \quad \left(\frac{€}{yr}\right) = r_{exchange} * CAPEX \quad \left(\frac{\$}{yr}\right) \tag{C.4}$$

The CAPEX calculation forms the target function for the hydraulic design optimization. Operational costs are calculated from the reboiler duties of the distillation column(s), assuming 8000 operational hours per year, together with 10% of the purchase cost annually for maintenance:

$$OPEX \quad \left(\frac{€}{yr}\right) = Q_{reboiler}\left(\frac{GJ}{yr}\right) * 2.6GJ \Big/ ton * €24 \Big/ ton + 0.1 * \quad C_{purchase} \tag{C.5}$$

Together with the CAPEX this yields the total annualized cost (TAC (€/yr.)) for the flowsheets, which forms the target function for the flowsheet optimization:

$$TAC\left(\frac{€}{yr}\right) = CAPEX + OPEX \tag{C.6}$$

Appendix D. CAPEX cost item sizing

Column shell sizing

To determine the capital cost of the distillation column shell, the vessel weight is calculated as the defining size parameter. The column shell is sized as a vertical cylindrical pressure vessel with 2:1 elliptical heads (Seider et al., 2008). Note that equations D.1-D.6 use imperial units and the obtained vessel weight is converted to kilograms in the end. The operating pressure for the vessels in this work is 1 bara, which leads to a recommended design pressure P_d of 10 psig (recommended value for unit operating between 0 and 5 psig (Seider et al., 2008)).

The thickness of the vessel is calculated to withstand the internal pressure:

$$t_p = \frac{P_d D_i}{2SE - 1.2P_d} \tag{D.1}$$

Where the allowable stress is 15000 psi (based on the operating temperature (Seider et al., 2008)) and the welding efficiency, *E*, is taken to be 1. The wall thickness and the internal diameter (equals the tray diameter) are in inches. For low pressures equation D.1 might underestimate the thickness requirement for sufficient rigidity, so the minimum wall thicknesses shown in Table D-1 are imposed based on the internal column diameter.

Table D-1
Minimum wall thickness for vertical pressure vessels [20].

Vessel inside diameter (ft.)	Minimum wall thickness (in.)
Up to 4	**1/4**
4–6	**5/16**
6–8	**3/8**
8–10	**7/16**
10–12	**1/2**

Additionally, the vessel is also sized to withstand a substantial wind load of 140 miles/h with the required vessel thickness at the bottom calculated as:

$$t_w = \frac{0.22(D_o + 18)L_c^2}{SD_o^2} \tag{D.2}$$

Where the term 18 accounts for column cage ladders. D_o is the outer diameter of the vessel ($D_i + t_p$) The averaged (between top and bottom) wall thickness is then:

$$t_v = t_p + 0.5t_w \tag{D.3}$$

Finally, a corrosion allowance is added on top of the vessel thickness to arrive at the shell thickness:

$$t_s = t_v + \frac{1}{8}in. \tag{D.4}$$

Taking into account that fabrication of the shell comes from metal plate that is available in fixed increments, t_s is rounded upwards to the nearest available size, given in Table D-2.

Table D-2
Shell material thickness availability.

Size range (in.)	Increment (in.)
3/16 – 1/2	**1/16**
5/8–2	**1/8**
2 ¼ - 3	**1/4**

The vessel length is determined from the number of separation stages, N_s, and additional sizing allowance for disengagement height and sump height:

$$L_c = ((N_s * TS) + L_{de} + L_{sump}) * 3.28ft./m \tag{D.5}$$

Where the disengagement height is set at 1.2 m and the sump height is set at 3 m. Note that the column length is converted to ft. With all size parameters of the vessel now known, the vessel weight can be calculated:

$$W = \pi(D_i + t_s)(L_c + 0.8D_i)t_s\rho \tag{D.6}$$

Where the term $0.8D_i$ accounts for the elliptical heads of the column. The density of steel is taken to be 490 lb/ft^3. Finally, the vessel weight is converted to kilograms with the conversion rate of 1 kg = 0.4535 lb.

Heat exchanger sizing

To determine the capital cost of the condenser and reboiler heat exchangers, the heat exchange area is calculated as the defining size parameter. A constant temperature gradient of 20 K is assumed for both the condenser and reboiler, this is done to decouple the heat exchanger sizing from the relative volatility of the components in preparation for future work. The heat exchange area is calculated as follows:

$$A_{C,tot} = \frac{Q_C}{U_C * \Delta T_C} \tag{D.7}$$

$$A_{R,tot} = \frac{Q_R}{U_R * \Delta T_R} \tag{D.8}$$

Where the values for the heat transfer coefficients are $U_C = 850$ W/m^2 K (organic vapors → water) and $U_R = 600$ W/m^2 K (steam → light organics). To take the validity limits of the cost correlation into account (500 m^2 for the condenser, 1000 m^2 for the reboiler), the calculated heat exchange area is divided over multiple heat exchangers if the maximum area for a single heat exchanger is surpassed:

$$if \quad A_{C,tot} > A_{C,\max}, N_{Cond} = ceil(\frac{A_{C,tot}}{A_{C,\max}}) \tag{D.9}$$

$$if \quad A_{R,tot} > A_{R,\max}, N_{Reb} = ceil(\frac{A_{R,tot}}{A_{R,\max}}) \tag{D.10}$$

Where *ceil* is a MATLAB function that takes the input and rounds it up to the nearest integer i.e., producing an integer number of heat exchangers. The heat exchange area per heat exchanger then becomes:

$$A_C = A_{C,tot}/N_{Cond} \tag{D.11}$$

$$A_R = A_{R,tot}/N_{Reb} \tag{D.12}$$

Appendix E. Hydraulic sub-model

Effective froth density

The frothy liquid pool held on the trays is significantly aerated by the passing vapor stream. Since liquid residence time, or holdup, is a key parameter to design for adequate reaction performance, obtaining a good estimate of the effective froth density on the trays is important in RD column design. Several empirical froth density models are available in open literature, notably Colwell's method and the correlation by Bennett et al. (1983);

Colwell (1981). Both models incorporate an inverse relation between the gas velocity and the froth density. Note that these models were originally developed to predict pressure drop through the liquid pool, rather than liquid holdup for reaction residence time. In this work the correlation by Bennett, Agrawal and Cook is used since it is the only model for which coefficients for both sieve and bubble cap trays have been published (Shenastaghi et al., 2018), see Table E-1.

The froth density is given by:

$$\phi_e = e^{-C_4 K_S} \tag{E.1}$$

Where

$$K_S = U_a \left(\frac{\rho_V}{\rho_L - \rho_V} \right)^{C_5} \tag{E.2}$$

The clear liquid height is the sum of the liquid held by the weir and the liquid crest over the weir:

$$h_c = \phi_e \left[h_w + C_l \left(\frac{Q_L}{L_w \phi_e} \right)^{2/3} \right] \tag{E.3}$$

Where

$$C_l = C_1 + C_2 e^{-C_3 h_w} \tag{E.4}$$

Table E-1
Froth density and clear liquid height model coefficients (Bennett et al., 1983; Shenastaghi et al., 2018).

Coefficient	Sieve tray	Bubble cap tray
C_1	0.03272	0.312
C_2	0.02865	3.303
C_3	137.8	62.32
C_4	12.55	2.069
C_5	0.91	0.43

Hydraulic sub-model implementation

An overview of the tray design parameters is shown in Table E-2. The imposed limits of these parameters are based on values reported in open literature that have been known to be applied in existing columns and/or have been shown experimentally to not adversely affect separation efficiency to a significant degree (Kister et al., 2019).

Tray spacing for medium fouling services is not recommended to be below 18 in./0.45 m for medium sized towers (i.e., >5 ft./1.5 m diameter), 15 in./0.38 m is mentioned as the lower end for chemical towers with < 5 ft./1.5 m diameter, with some applications going as low as 0.3 m. Do note however, that such a small tray spacing is only chosen when there is a solid knowledge base on the performance of the specific application and/or there is a strong economic incentive to limit column height (e.g. fitting in a cold box or site-specific height regulations) (Kister, 1990).

Table E-2
Tray design parameters and applied ranges.

Design param.	Symbol	Units	Range	Related hydraulic phenomena	Notes
Tray spacing	*TS*	m	0.4 * –0.9 m. (16–36 in.)	Entrainment, downcomer backup flood	Set either by entrainment over the active bubbling area or the backup of frothy liquid in the downcomer.
Fraction of flooding	f_{flood}	(-)	0.4–0.8	Entrainment, weeping	Sets the column diameter.
Tray open area	A_G/A_B	(-)	0.08–0.14	Weeping, downcomer backup flood	Sets the vapor velocity through the disperser unit.

*Rounded up from 0.38 m since optimization designs tray spacing in 0.05 m increments.

Little is published about operating with high weir heights/deep liquid pools on trays. As such, this presents a significant uncertainty when designing high holdup trays for homogeneous reactive distillation. Furthermore, the underlying data sets for entrainment, weeping and flooding only contain experimentally measured points with trays up to 0.1 m weirs and mostly air/water as fluid mixture. A single study using up to 0.9 m weirs (Haug, 1976) reports data that suggests that the known weeping prediction methods overestimate weeping at weir heights outside of the typical ranges. By necessity, extrapolating the tray design rules to high weir heights has to be approached with due diligence.

The fraction of flooding is conventionally kept high, around 80%, to minimize investment costs and liquid holdup. Taking 80% of flooding velocity as the normal operating value, a trays' turndown ratio gives the lower limit for the vapor velocity at which efficiency is maintained, below which non-uniform vapor flow through the liquid pool and/or excessive weeping occurs resulting in poor vapor-liquid contact (Kister et al., 2019).

The tray open area is to be kept between 8 % and 14 % to maintain separation efficiency and operability for sieve trays (Kister et al., 2019). For the bubble cap trays, open area is not pre-set but is a result of populating the active tray area with the maximum amount of bubble caps possible with fixed

dimensions in a triangular pitch with the cap lanes normal to liquid flow. The dimensions are set to the recommended values for general-purpose bubble caps by Bolles, shown in Table E-3 (Coker, 2011).

Table E-3
Dimensions for all-purpose bubble-caps as recommended by Bolles [32]. Conversion of 1 in. = 25.4 mm used in calculations.

Design parameter	*Value*
Cap dimensions	
Cap outer diameter	4 in. (101.6 mm)
Cap inner diameter	3 7/8 in. (98.4 mm)
Riser outer diameter	2.75 in. (69.9 mm)
Riser inner diameter	2.68 in. (68.1 mm)
Skirt clearance	¼ in. (6.4 mm)
Slot dimensions	50
Number of slots/cap	1.5 in. (38.1 mm)
Slot height	1/8 in. (3.2 mm)
Slot width	
Cap spacings	
Cap to Cap	1.5 in. (38.1 mm)
Cap to Wall	1.5 in. (38.1 mm)
Cap to Weir	3 in. (76.2 mm)

The hydraulic phenomena that limit stable tray operation are weeping (sieve trays only), liquid entrainment and downcomer backup flooding. The recommended limits for these phenomena (Coker, 2011; Kister et al., 2019; Seider et al., 2008) form a set of constraints for the tray optimization:

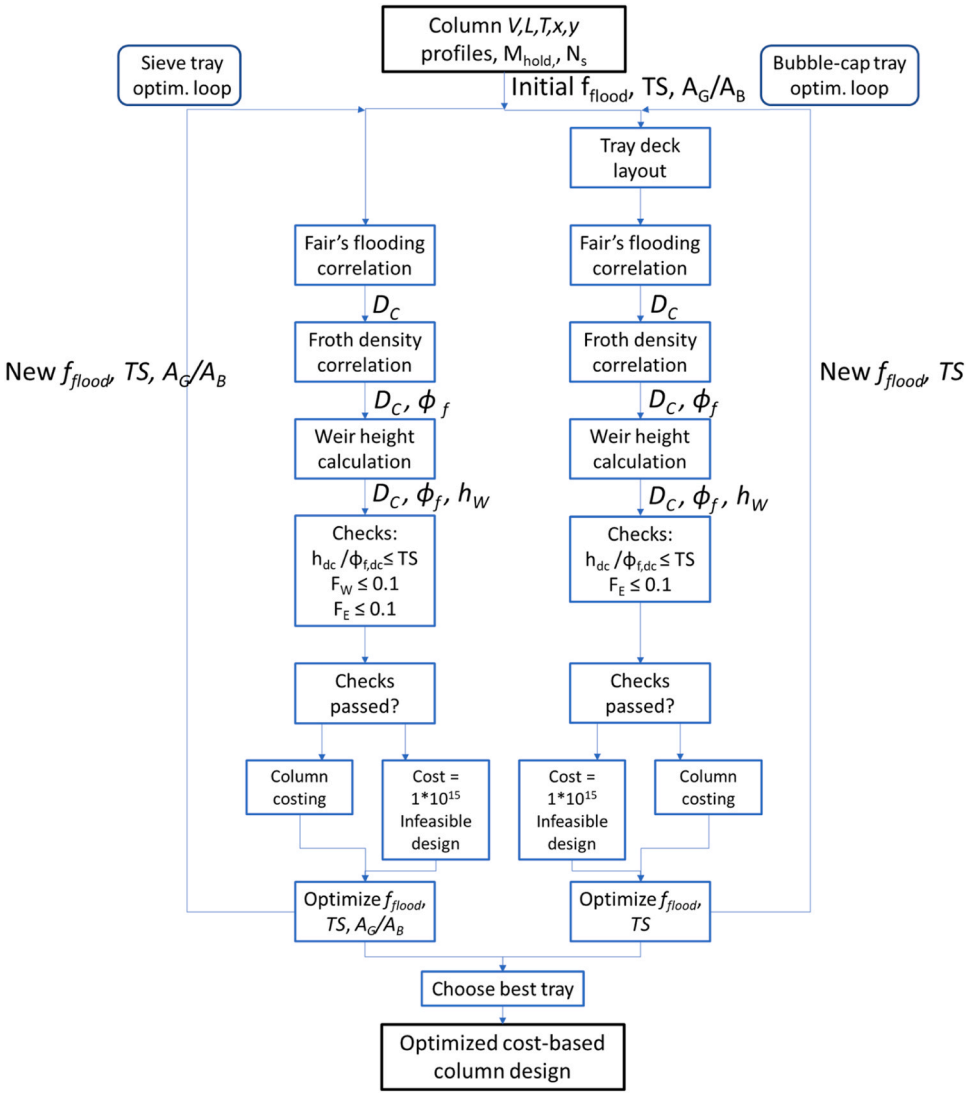

Fig. 7. Hydraulic optimization algorithm for column design.

$$f_E \leq 0.1 \tag{E.5}$$

$$\frac{h_{dc}}{\phi_{f,dc}} \leq TS \tag{E.6}$$

$$f_W \leq 0.1 (\text{sieve trays only}) \tag{E.7}$$

These are evaluated according to the procedures reported in an earlier work [19]. Optimization achieves a single tray design where these constraints are evaluated for every reactive tray in the RD columns and every tray in the normal distillation columns. For RD, the rectifying and stripping stages are of the same tray type, diameter and tray spacing as the reactive trays but with 5 cm. weirs. If any constraint is violated then the cost value of that set of optimization parameters is set to $\$1 \bullet 10^{15}$. The optimization problem is solved using MATLAB's built in Simulated Annealing (SA) solver. The settings for the solver are given in Appendix E. A schematic layout of the hydraulic optimization routine is given in Fig. 7.

References

Agreda, V.H., Partin, L.R., Heise, W.H., 1990. High-purity methyl acetate via reactive distillation. Chem. Eng. Prog. 86, 40–46.

Barbosa, D., Doherty, M.F., 1988a. The simple distillation of homogeneous reactive mixtures. Chem. Eng. Sci. 43, 541–550. https://doi.org/10.1016/0009-2509(88)87015-5.

Barbosa, D., Doherty, M.F., 1988b. The influence of equilibrium chemical reactions on vapor—liquid phase diagrams. Chem. Eng. Sci. 43, 529–540. https://doi.org/10.1016/0009-2509(88)87014-3.

Baur, R., Krishna, R., 2004. Distillation column with reactive pump arounds: an alternative to reactive distillation. Chem. Eng. Process.: Process.Intensif. 43, 435–445. https://doi.org/10.1016/S0255-2701(03)00128-4.

Bennett, D.L., Agrawal, R., Cook, P.J., 1983. New pressure drop correlation for sieve tray distillation columns. AIChE J. 29, 434–442. https://doi.org/10.1002/aic.690290313.

Bessling, B., Schembecker, G., Simmrock, K.H., 1997. Design of processes with reactive distillation line diagrams. Ind. Eng. Chem. Res 36, 3032–3042. https://doi.org/10.1021/ie960727p.

Blahušiak, M., Kiss, A.A., Babic, K., Kersten, S.R.A., Bargeman, G., Schuur, B., 2018. Insights into the selection and design of fluid separation processes. Sep Purif. Technol. 194, 301–318. https://doi.org/10.1016/J.SEPPUR.2017.10.026.

Cardoso, M.F., Salcedo, R.L., De Azevedo, S.F., Barbosa, D., 2000. Optimization of reactive distillation processes with simulated annealing. Chem. Eng. Sci. 55, 5059–5078. https://doi.org/10.1016/S0009-2509(00)00119-6.

Ciric, A.R., Gu, D., 1994. Synthesis of nonequilibrium reactive distillation processes by MINLP optimization. AIChE J. 40, 1479–1487. https://doi.org/10.1002/aic.690400907.

Coker, A.K., 2011. Ludwig's applied process design for chemical and petrochemical plants, Ludwig's Applied Process Design for Chemical and Petrochemical Plants. Elsevier Science.

Colwell, C.J., 1981. Clear liquid height and froth density on sieve trays. Ind. Eng. Chem. Process Des. Dev. 20, 298–307. https://doi.org/10.1021/i200013a019.

Harmsen, G.J., 2007. Reactive distillation: The front-runner of industrial process intensification: a full review of commercial applications, research, scale-up, design and operation. Chem. Eng. Process.: Process.Intensif. 46, 774–780. https://doi.org/10.1016/j.cep.2007.06.005.

Haug, H.F., 1976. Stability of sieve trays with high overflow weirs. Chem. Eng. Sci. 31, 295–307. https://doi.org/10.1016/0009-2509(76)85075-0.

Kiss, A.A., Segovia-Hernández, J.G., Bildea, C.S., Miranda-Galindo, E.Y., Hernández, S., 2012. Reactive DWC leading the way to FAME and fortune. Fuel 95, 352–359. https://doi.org/10.1016/J.FUEL.2011.12.064.

Kister, H.Z., 1990. Distillation Operation. 's AccessEngineering. McGraw-Hill Education. McGraw-Hill,.

Kister, H.Z., Matthias, P.M., Steinmeyer, D.E., Penney, W.R., Monical, V.S., Fair, J.R., 2019. Equipment for distillation, gas absorption, phase dispersion, and phase separation. Perry's Chemical Engineers' Handbook. McGraw-Hill Education, NY.

Levenspiel, O., 1999. Chemical Reaction Engineering. Wiley,.

Lucia, A., 2008. Chemical engineering design principles, practice, and economics of plant and process design By G. Towler and R. Sinnott. AIChE J. 54, 3034–3035. https://doi.org/10.1002/aic.11633.

Luyben, W.L., Yu, C.C., 2009. Reactive Distillation Design and Control. Wiley,.

Malone, M.F., Doherty, M.F., 2000. Reactive distillation. Ind. Eng. Chem. Res 39, 3953–3957. https://doi.org/10.1021/ie000633m.

Muthia, R., Reijneveld, A.G.T., van der Ham, A.G.J., ten Kate, A.J.B., Bargeman, G., Kersten, S.R.A., Kiss, A.A., 2018. Novel method for mapping the applicability of reactive distillation. Chem. Eng. Process. - Process. Intensif. 128, 263–275. https://doi.org/10.1016/J.CEP.2018.04.001.

Naphtali, L.M., Sandholm, D.P., 1971. Multicomponent separation calculations by linearization. AIChE J. 17, 148–153. https://doi.org/10.1002/aic.690170130.

Noll, L., Ham, L., Oudenhoven, S., ten Kate, A., Bargeman, G., Kersten, S., 2023. Extension of the equilibrium stage model to include rigorous liquid holdup calculations for reactive distillation. Processes 11, 1131. https://doi.org/10.3390/pr11041131.

Schembecker, G., Tlatlik, S., 2003. Process synthesis for reactive separations. Chem. Eng. Process.: Process.Intensif. 42, 179–189. https://doi.org/10.1016/S0255-2701(02)00087-9.

Segovia-Hernández, J.G., Hernández, S., Bonilla Petriciolet, A., 2015. Reactive distillation: a review of optimal design using deterministic and stochastic techniques. Chem. Eng. Process.: Process.Intensif. 97, 134–143. https://doi.org/10.1016/J.CEP.2015.09.004.

Seider, W.D., Seader, J.D., Lewin, D.R., Widagdo, S., 2008. Product and Process Design Principles: Synthesis, Analysis and Design. Wiley,.

Shenastaghi, F.K., Roshdi, S., Kasiri, N., Hasan Khanof, M., 2018. CFD simulation and experimental validation of bubble cap tray hydrodynamics. Sep Purif. Technol. 192, 110–122. https://doi.org/10.1016/J.SEPPUR.2017.09.055.

Taylor, R., Krishna, R., 2000. Modelling reactive distillation. Chem. Eng. Sci. 55, 5183–5229. https://doi.org/10.1016/S0009-2509(00)00120-2.

Thery, R., Meyer, X.M., Joulia, X., Meyer, M., 2005. Preliminary design of reactive distillation columns. Chem. Eng. Res. Des. 83, 379–400. https://doi.org/10.1205/CHERD.04112.

Théry-Hétreux, R., Meyer, X.Mi, Meyer, M., Joulia, X., Brehelin, M., Amoros, D., 2012. Feasibility analysis, synthesis, and design of reactive distillation processes: a focus on double-feed processes. AIChE J. 58, 2346–2356. https://doi.org/10.1002/aic.12768.

Tsatse, A., Oudenhoven, S.R.G., ten Kate, A.J.B., Sorensen, E., 2021. Optimal design and operation of reactive distillation systems based on a superstructure methodology. Chem. Eng. Res. Des. 170, 107–133. https://doi.org/10.1016/J.CHERD.2021.03.017.

Tung, S.-T., Yu, C.-C., 2007. Effects of relative volatility ranking to the design of reactive distillation. AIChE J. 53, 1278–1297. https://doi.org/10.1002/aic.11168.

Venimadhavan, G., Malone, M.F., Doherty, M.F., 1999. Bifurcation study of kinetic effects in reactive distillation. AIChE J. 45, 546–556. https://doi.org/10.1002/aic.690450311.